1959BAICz..10..149V

БЮЛЛЕТЕНЬ АСТРОНОМИЧЕСКИХ ИНСТИТУТОВ ЧЕХОСЛОВАКИИ
1 сентября 1959 г. Том 10 № 5

BULLETIN OF THE ASTRONOMICAL INSTITUTES OF CZECHOSLOVAKIA
1959, September 1. Volume 10 No 5

THE FLARE SPECTROGRAPH AT ONDŘEJOV

B. Valníček, V. Letfus, M. Blaha, Z. Švestka and *Z. Seidl*, Astronomical Institute of the Czechoslovak Academy, Ondřejov

Received February 18, 1959.

This Paper presents a description of the new solar spectrograph built at the Ondřejov Observatory in the year 1958. The spectrograph enables to take a series of simultaneous photographs of several spectral regions in short time intervals with a dispersion of at least 1 Å/mm, so that it is highly suitable for the study of chromospheric flares and active prominences.

Большой спектрограф для наблюдения вспышек в Ондржейове. В статье приводится описание конструкции нового солнечного спектрографа, построенного в 1958 году в Ондржейовской обсерватории. С помощью прибора можно получить спектры хромосферных вспышек в нескольких спектральных областях с дисперсией 1 Å/мм или больше, причем несколько областей экспонируются одновременно. Экспозиции могут осуществляться в коротких последовательных интервалах времени, так что приведенный спектрограф пригоден для прослеживания быстро изменяющихся явлений в солнечной атмосфере.

1. Introduction

One hundred years ago, in the year 1859, the first solar flare was observed by Carrington and Hodgson in England. Since that time, solar flares have attracted the attention of astronomers more and more, especially due to their evident connection with geomagnetic and ionospheric effects on the Earth. The enormously increased emission of short-wave radiation, cosmic rays, and corpuscules from flare areas on the Sun, together with their interesting rapid development, made the question on the cause of the flare appearance one of the most interesting problems of solar physics.

When discussing this problem, the most promising way manifests itself in a study of flare spectra, which are characterized by emission lines of hydrogen, absorption or emission lines of neutral helium, and reversals in the cores of lines of metals in low states of ionisation.

The first attemps at obtaining flare spectra were made by Richardson, Minkowski, and Allen [1, 2]. Their studies discovered the general character of the flare emission, but the qualitative results were not adequate for any theoretical discussion of the physical structure of flares.

Therefore, after the second world war, several authors tried to get more quantitative results of flare spectra, especially in the form of photometric profiles of the emission lines. The pioneer work was made by Ellison, who obtained well-defined profiles of the H_α emission line for several flares in the years 1946—1951 [3]. In the year 1951, a profile of the H_{10} line was obtained for one flare by Suemoto [4]. These profiles were discussed in detail by one of the present writers [5], but, of course, isolated observations of only one emission line could not lead to any conclusive results.

In the year 1949, more progress was made, when Mustel and Severny at the Crimean Observatory obtained a series of spectra of the great flare of August 5, 1949, containing the Balmer H_α, H_γ, H_δ, H_ε, and H_ζ lines [6]. Since that time, Severny and his collaborators obtained several other spectra of flares and discussed profiles of the Balmer lines together with the $H + K$ lines of ionised calcium in a series of papers [7]. Nevertheless, all their results are open to some discussion, due to the fact that different lines were photographed at different times. It is clear that the rapid development of flares necessarily needs a simultaneous photograph of the whole flare spectrum. Any comparison of lines taken at different phases of the development of a flare, as has been made by Severny, may obviously lead to erroneous results. Moreover, we can never be sure that at two different times exactly the same point of the flare is set on the slit of the spectrograph. With regard to the fine detailed structure of emitting knots of the flare, any even slight change of position may be a source of another serious error if the photography of all investigated lines is not simultaneous. And, in the third place, the resulting line profiles and especially the recorded form of the extension of wings (moustaches) are very sensitive to the air conditions at the moment of exposure. If all the lines are not taken in the same moment, the influence of air disturbances may be different at different lines, which causes a further source of inexactitude.

Thus we come to the conclusion that only simultaneous photographs of various emission lines in the flare spectrum

Publishing House of the Czechoslovak Academy of Sciences • Provided by the NASA Astrophysics Data System

1959BAICz..10..149V

can bring reliable informations about the physical conditions in flares.

Flare spectrographs which fulfil this basic condition have been built in the most recent time at several solar observatories. A report has already been given on the spectrograph on Pic du Midi [8], and some spectra were presented by American and Japanese astronomers at the General Assembly of I. A. U. in Moscow in August, 1958. At this meeting we also presented some examples of spectra obtained by the new flare spectrograph built at the Ondřejov Observatory. A detailed description of this equipment is the subject of the presented paper.

2. General Conception

At the construction of the Ondřejov flare spectrograph we aimed to fulfil the following necessary conditions:

(a) The dispersion must be of the order of 1 Å/mm.

(b) The photographed spectrum has to cover lines of the Balmer series, some helium lines, H and K lines, and some important multiplets of iron and other metals.

(c) More parts of the spectrum must be taken simultaneously.

(d) The spectrograph has to enable the observer to get a series of spectra in short time-intervals to cover the whole development of flares.

(e) The focal image of the Sun must be as large as possible to enable the distinguishing of fine details in the flare structure. On the other hand, the exposures must be shorter than one second to diminish the influence of air disturbances as much as possible.

(f) The spectrograph must be in close connection with visual flare patrol to be able to catch the most interesting premaximum and maximum phases of the flare development.

These requirements were fulfilled in the following way:

(a) The dispersion in 5 spectral regions is the same and equals 1 Å/mm, in 2 remaining UV regions it is 0·67 Å/mm.

(b) Generally there are two alternatives: either to expose broad regions of the spectrum on long sections of film as has been done by Michard [8] for instance, or to restrict oneself to small portions of the spectrum only, with the most interesting spectral lines, using photographic plates. We chose the second alternative for three main reasons: firstly, it is much easier to form a perfect image of a short spectral region than to focus a broad part of the spectrum with a satisfactory dispersion; secondly, the emulsion on plates is generally more homogeneous and thus enables more precise photometric work; and, in the third place, due to the change of intensity along the solar spectrum, it is rather difficult to get the correct density along the whole spectral region photographed on a long section of film.

The selected spectral regions include the following important lines:

Plate 1	λ 6503 — λ 6623	includes the H_α line of hydrogen
Plate 2	λ 5829 — λ 5949	includes the D lines of sodium and the D_3 line of helium
Plate 3	λ 4797 — λ 4917	includes the H_β line of hydrogen
Plate 4	λ 4277 — λ 4397	includes the H_γ line of hydrogen, 5 lines of the 41st multiplet of Fe I, 3 lines of the 27th multiplet of Fe II, and 10 lines of the 44th multiplet of Ti I
Plate 5	λ 3870 — λ 3990	includes the H_ε and H_ζ lines of hydrogen, the H and K lines of Ca II, λ 3964·7 line of He I, λ 3905·5 line of Si I, 9 lines of the 4th multiplet of Fe I, 5 lines of the 20th multiplet of Fe I, both lines of the first multiplet of Al I, and all 8 lines of the 15th multiplet od Ti I
Plates 6 and 7	λ 3640 — λ 3814	include the higher Balmer lines from H_{10} up to the series limit, 12 lines of the 5th multiplet of Fe I, 2 lines of the 14th multiplet of Ti II and 2 lines of the 3rd multiplet of Ca II.

(c) Due to very great differences of intensity all 7 plates cannot be exposed by means of one single exposure. Only the plates 1—5 can be taken simultaneously, while for the remaining plates 6 and 7 a longer exposure time is necessary. The exposure is made by a shutter on the slit. The differences of intensity in the spectral regions 1—5 are levelled by a suitable choice of plates and developers.

(d) Twelve spectra and two photometric scales may be exposed on one plate. The shift of plates can be done either individually or by means of an automatic adjustment, to which the exposure time and the time intervals between successive exposures can be prescribed. The shortest possible time interval between two subsequent exposures equals 10 seconds. When the set of 12 exposures is finished, all plate-holders return automatically to the starting position. During the return time, which lasts less than one minute, the plates can be changed and another series of spectra is ready to be started.

(e) The focal image of the Sun has a mean diameter of 125·6 mm. In different spectral regions 1 mm of the vertical scale of the spectrum corresponds to 17·3″ up to 23·6″ on the solar disc. The exposure time varies between 1/25 and 1 second for plates Nos. 1—5 and 5 to 10 seconds for plates Nos. 6 and 7, according to the height of the Sun above the horizon, the transparency of the air, and the seeing conditions.

(f) All the time when the spectrograph is prepared to work, the chromosphere is observed in short time intervals (3—5 minutes) in the spectrohelioscope. The observer in the spectrohelioscope is connected by means of a loud telephone with the worker in the spectrograph.

Publishing House of the Czechoslovak Academy of Sciences • Provided by the NASA Astrophysics Data System

1959BAICz..10..149V

Thus any appearance of a chromospheric flare tohether with its position is immediately known and the exposures in the spectrograph can be started.

3. General Description

The spectrograph is placed in a room of dimensions 18 times 9 meters, which is situated in the first storey of the main building of the observatory. The floor is double. The lower floor carries the supporting pillars observer (R_o) and enters the room of the spectrograph proper (R_s). In this second room the solar light falls first on the collimator mirror (K) of 230 mm diameter and 850 cm focal length. The collimator optical axis contains an angle of 44′ with the straight line connecting the centres of the collimator and the slit. After that the second plane mirror (M_2) reflects the light to the grating (G). The angle of incidence on the grating is 1°33′.

The grating made by G. O. I. in the U. S. S. R. has 600 lines·per mm and its size is 90 times 100 mm, with

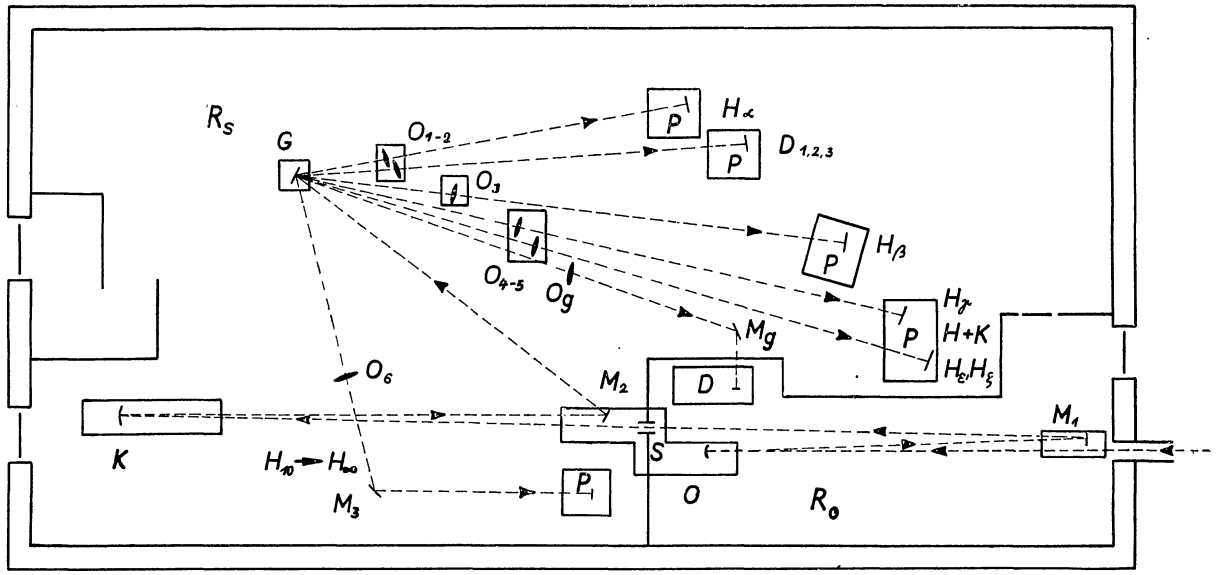

Fig. 1. Scheme of the spectrograph: R_0 = room of the observer, R_s = room of the proper spectrograph, O = objective mirror, S = slit of the spectrograph in the imaging plane of the objective mirror, K = collimator mirror, G = grating, O_{1-2} = imaging objectives of the H_α and D regions, O_3 = imaging objective for the H_β region, O_{4-5} = imaging objectives for the H_γ and $H+K$ regions, O_6 = imaging objective for the UV region, P = plate holders, O_g = objective for the H_α line in the first order used to guiding, D = control desc of the observer.

and the upper one is separated from all elements of the optical system. Moreover, to prevent any possible sources of shocks, red alarm lights are switched on in all other rooms and corridors of the building as soon as the photographic mechanism of the spectrograph is put in action.

The solar light is cast into this room by a coelostat situated on a tower detached from the main building. Mirror diameters of the coelostat are 360 and 280 mm. The coelostat is covered by a cylindrical double roof with very good thermic isolation. This roof can be shifted on rails close to the southern wall of the building, so that any turbulent motions in the close vicinity of the wall cannot disturb the optical path of the solar beams.

The general scheme of the spectrograph is shown in Fig. 1. The solar beam coming from the coelostat falls on the objective spheric mirror (O) of 230 mm diameter and 1350 cm focal length. After a reflexion on the plane mirror (M_1) the objective forms a focal image of the Sun (125·6 mm in diameter) in the plane of the slit (S). The angle between the optical axis of the objective mirror and the straight line connecting the centres of the objective (O) and the mirror (M_1) is 1°10′. The height of the slit is 50 mm and its usual working width is 0·0534 mm. The height of the slit used at the exposures of a flare spectrum is 20 mm.

On the slit the solar beam leaves the room of the the maximum concentration of light into the right second order. Five spectral regions are photographed in the second order on the right-hand side and two regions in the third order on the left-hand side of the grating.

Spectra on the right-hand side are formed by five objectives (O_{1-5}). The focal lengths of these objectives were calculated in such a way that the linear dispersion in all five spectral regions equals 1 Å/mm. Four objectives imaging the surrounding of the H_α, $D_{1,2}$, H_β, and H_γ lines are single lenses corrected for the spherical aberration, the fifth one, for the region of the H_ε, H, K, and H_ζ lines is a double objective corrected for the spherical and chromatic aberration. All these objectives were made by the Institute for Fine Mechanics and Optics in Přerov, while the basic mirror system was made in the Institute for Minerals in Turnov.

Spectra on the left-hand side are formed by a common objective (O_6). It is a UV double Zeiss objective and it is used for the higher members of the Balmer series up to the Balmer continuum and this range of the spectrum is photographed after the reflexion on the mirror (M_3) on two plates, one close to the other, with a linear dispersion of 0·67 Å/mm.

The following Table gives the diameters and focal lengths of the Objectives O_{1-6}, linear dispersions, angular

Publishing House of the Czechoslovak Academy of Sciences • Provided by the NASA Astrophysics Data System

1959BAICz..10..149V

dimensions of the parts of the solar disc corresponding to 1 mm height of the spectrum, and the types of Schott-filters placed in front of the plates.

Table 1

Objective	Plate No.	∅ (mm)	f (cm)	Linear dispersion (Å/mm)	1 mm corresponds to	Filter
O_1	1	130	550	1·00	23·6″	OG 3
O_2	2	130	620	1·00	21·0	GG 7
O_3	3	140	700	1·00	18·7	WG1
O_4	4	143	725	1·00	17·9	—
O_5	5	160	750	1·00	17·3	—
O_6	6,7	240	600	0·67	21·7	BG25

All 7 spectral regions are photographed on plates 130 times 180 mm, in their vertical position. The plate holders (P) can be electrically shifted in the vertical direction in suitable intervals, which are chosen by an appropriate setting of movable electric contacts. A diaphragm in front of the plate holder determines the height of the photographed spectrum. Usually a heigt of 10 mm is used, which corresponds to 0·09 up to 0·12 of the solar diameter. Then twelve spectra can be obtained on one plate, together with two photographs of a photometric scale on the upper and lower ends of the plate. To diminish the influence of scattered light and to eliminate the light from the other orders, colour filters are put before the plates. The list of filters used is given in Table 1. The filters are slightly inclined towards the optical axis (5°) to eliminate any interference phenomena which might appear at the perpendicular incidence of the light beams. The intensity of secondary reflexions on the filters will be discussed in the 10th paragraph.

The photometric scale is formed by a set of 9 layers of evaporated platinum. It is put on the slit after the finished exposures and illuminated by the centre of the solar disc. The total height of the scale is 7 mm, which corresponds only to 0·056 of the diameter of the solar image, so that the limb variation of the intensity is without any influence. To eliminate any possible influence of a wedge shape of the slit (which, however, is very small, as will be shown in the 6th paragraph), the slit is broadened to 0·16 mm and 0·31 mm respectively when exposing the scale, while the intensity of the solar light is reduced by a neutral Schott NG 5 — filter placed in front on the slit. The scale exposure is the same as during the photographs of the spectrum. During the set of normal photographs of the spectrum the scale is replaced on the slit by two marks, which form on all spectra two horizontal lines, to which all vertical distances in the spectrum can be referred.

Exposures of the spectral regions 1—5 are made at the same moment, by means of a shutter which is placed close behind the slit. The plates 6 and 7 are exposed automatically immediately after that. In addition to the shutter close to the slit, there are individual shutters in front of all plate holders, which cover the plates when photographs of other spectral regions are taken and during the time between exposures. These shutters permit the main shutter to keep open during that time, so that the spectrum can be observed and the flare guided visually between the successive photographs.

In the year 1958 only exposures in the spectral regions 1—5 were made, the arrangement of the remaining regions 6 and 7 was not finished till in the year 1959.

To find the flare we use the H_α line in the first order on the right-hand side of the grating. An objective (O_g) and a system of mirrors (M_g) form the image of the H_α line in the level of the control desk (D) of the spectrograph, where the H_α line can be visually followed by means of an eyepiece.

The image of the Sun formed on the screen in the plane of the slit can be observed by means of another optical system in an eyepiece also placed over the control desk. Close in front of the screen a vertical wire can be moved in the horizontal direction. This movable wire can be set on a suitable well-defined sunspot rather far from the slit, and by means of this sunspot the solar image can be permanently guided.

When a flare and its approximate position is announced from the spectrohelioscope, the observer sets the flare on the slit of the spectrograph by means of the H_α-eyepiece. Then he sets the movable wire on a chosen sunspot and starts the exposures. This procedure lasts about 30 seconds. The combination of two guiding systems (H_α- and photospheric eyepiece) enables the flare to be kept exactly on the slit during the whole development of the flare, which cannot be made by the H_α-line guiding only. In the near future the guiding system will be supplemented by an H_α-monochromatic filter.

The guiding is made by electric movements of the coelostat mirror and more in detail by means of a turnable planparallel plate, which is placed in front of the slit. The various displacements of the solar image at different wave-lengths, due to the various index of refraction, are negligible when compared with the used width of the slit (0·0534 mm) and with regard to the size of the diffraction disc of the objective miror.

A system of relays in the observer's desk permits the carrying out of either individual exposures, or a series of exposures which follow one after the other in chosen time intervals and with prescribed exposure time. On pressing the start-button, the observer closes the main shutter on the slit, which enabled him up to the starting time to observe the emission features in the flare spectrum. Immediately after that the shutters in front of individual plate holders Nos. 1—5 are opened and the main shutter carries out the prescribed exposure. Then the shutters Nos. 1—5 are closed, Nos. 6 and 7 opened, and the main shutter makes exposure in these two regions. After that the individual shutters 6 and 7 are closed, the main shutter is re-opened, and the plate holders are shifted into the new position ready for the next exposure. The H_α line can be again visually observed. If, on the other hand, the automatic mechanism has been started, the whole procedure repeats after the chosen time-intervals. If the mechanism is not stopped during the set of exposures, the whole series of twelve spectra is successively carried out, and after that the plate holders return automatically into the starting position.

As an example, a complete set of twelve spectra in five spectral regions is shown in Fig. 2. It includes the main part of development of the great flare observed

Publishing House of the Czechoslovak Academy of Sciences • Provided by the NASA Astrophysics Data System

1959BAICz..10..149V

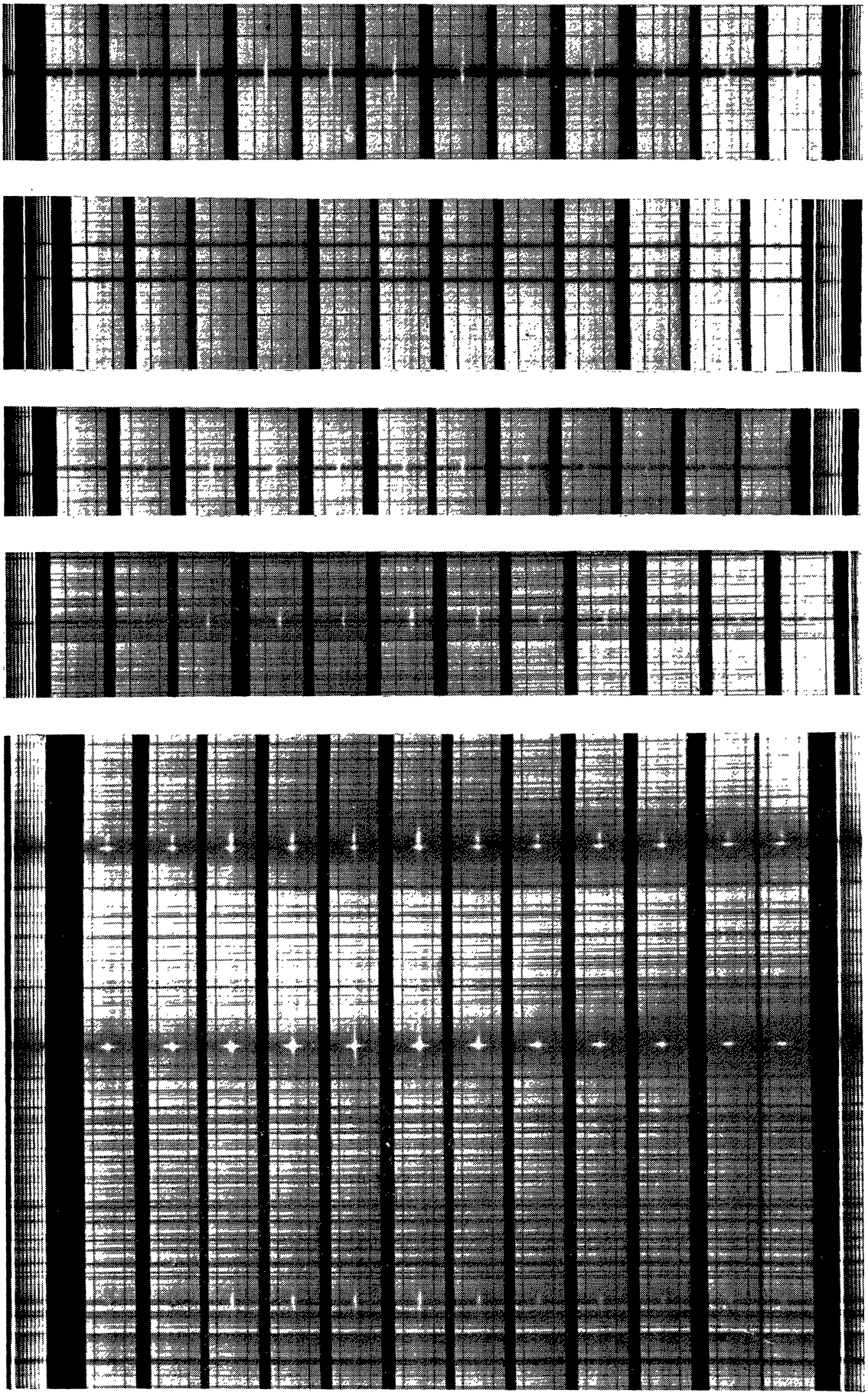

Fig. 2. Spectrum of the flare of July 20, 1958. Position 22 S, 66 W, imp. 2+. Exposure time 1 sec, the first exposure at $12^h07^m30^s$ U. T., intervals between successive exposures 1 minute.

Publishing House of the Czechoslovak Academy of Sciences • Provided by the NASA Astrophysics Data System

1959BAICz..10..149V

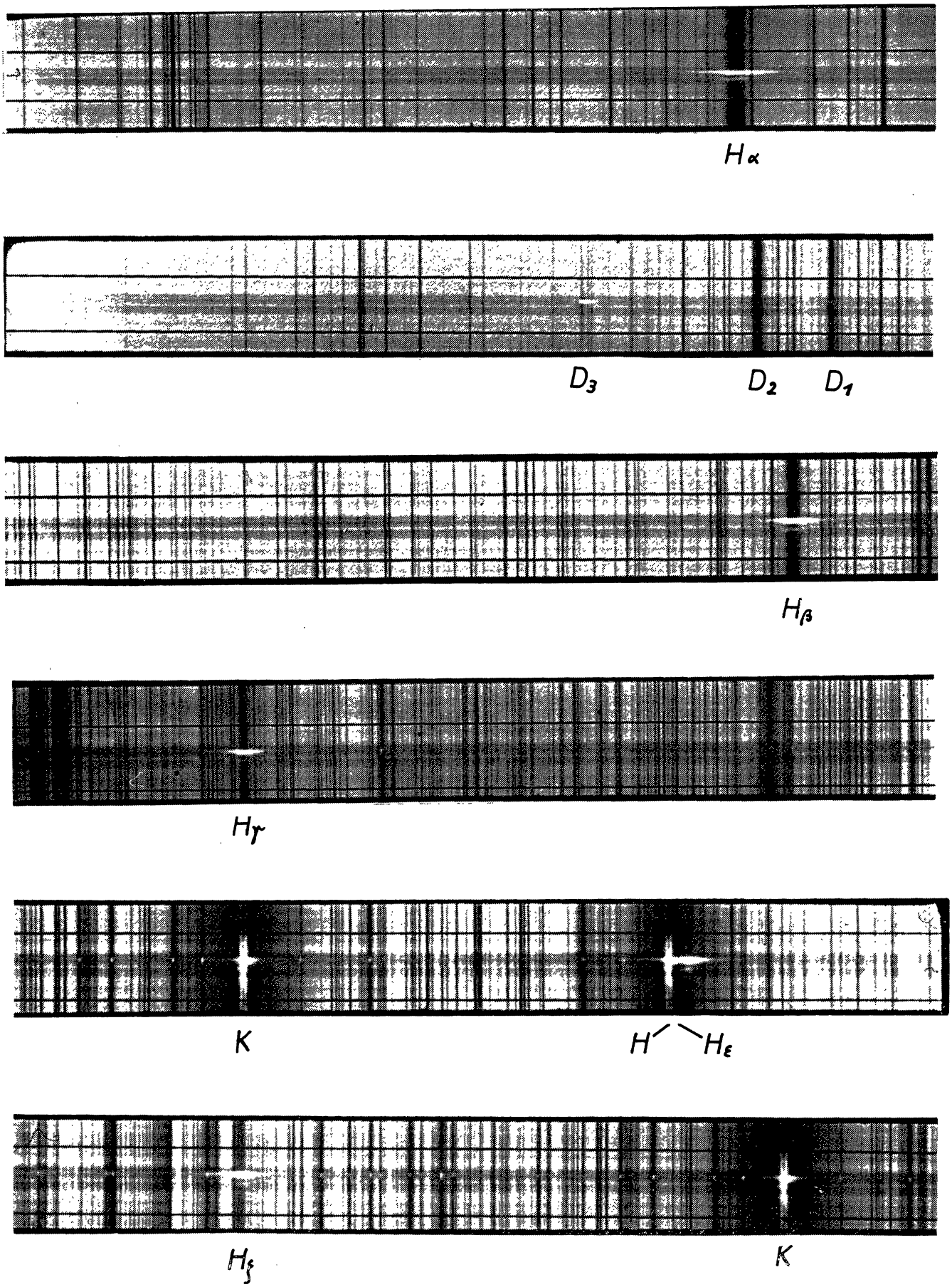

Fig. 4. Spectrum of the flare of July 30, 1958, $15^h38^m32^s$ U. T. Position 12 S, 64 W, imp. = 2. Exposure time 0·3 sec.

Publishing House of the Czechoslovak Academy of Sciences • Provided by the NASA Astrophysics Data System

1959BAICz..10..149V

on July 20, 1958, in the position 22 S and 66 W. The first spectrum was obtained at $12^h07^m30^s$ U. T., and the successive spectra were exposed in one minute intervals. The exposure time was one second. The course of emission can be compared with the curve of change of the effective H_α-line width as observed in the Ondřejov spectrohelioscope, shown in Fig. 3. The vertical segments denote the times of exposures of the presented flare spectra.

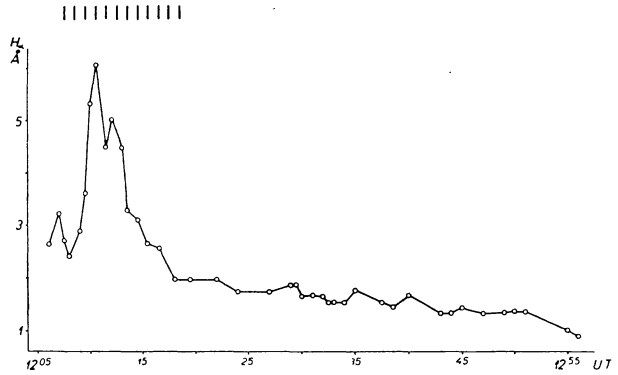

Fig. 3. The H_α effective line-width change of the flare from July 20, 1958, measured in the Ondřejov spectrohelioscope. Vertical segments denote times of exposures of the spectra, shown in Fig. 2.

Another example is shown in Fig. 4. In this case it was not possible to obtain a complete series of spectra due to cloudy weather.

4. *Photographic Process*

The exposure times of the spectrum vary according to the height of the Sun above the horizon, transparency of the air, and position of the photographed object on the solar disc. Their duration is determined by measuring the total illumination in front of the objective mirror.

For the plates Nos. 1, 3, 4, and 5, two kinds of developers are used: either the fine-grain D 76, if the task is to get a perfect picture of details in the spectrum and the seeing quality allows it, or Rodinal (1 : 20), which is more coarse-grained, but gives denser negatives, so that the exposure can be shorter. Such short exposures are necessary as soon as the seeing is not perfectly good, if we wish to get some details in the structure of the flare (moustaches, etc.). For the Astro panchromatic plate No. 2, which is exposed simultaneously with the plates 1, 3—5, only Rodinal is used, as the sensitivity of emulsion in rather small in this spectral region. The plates 6 and 7, which need substantially longer exposures, are exposed only in case of a perfectly quiet image of the sun. The following Table gives a summary of all kinds of plates, developers, and exposure times used.

At plates Nos. 3—7 the development process can be followed visually using a red safelight, at Nos. 1 and 2 the time of development is usually determined according to a test on a shred of the plate, or estimated according to the development time found at the plates Nos. 3—5.

The exposure times of prominence spectra in the regions 1—5 are in the range of 5—30 seconds, according to the brightness of the exposed phenomenon.

Table 2

Plate No.	1	2	3	4 5	6 7
Kind of plate	Agfa H_α	Agfa Astro Panchromatic	Agfa Spektral Blau Rapid	Agfa Astro or Spektral Blau Rapid	Afga Astro
Exposure time	0·04—0·5 sec				5—10 sec
Developer	Rodinal 1 : 20				
Exposure time	0·2—1·0 sec				
Developer	D 76	Rodinal	*D* 76	*D* 76	

5. *Calibration of the Photometric Scale*

The photometric scale was calibrated photographically: We exposed with constant exposure times the centre of the solar disc, with the scale on the slit, and screened the grating successively by rectangular diaphragms 8 times 8, 8 times 4, and 8 times 2 cm, respectively. All exposures were made three times on the same plate. Parts of the characteristic curve corresponding to individual steps of the scale were set together, and in this way the logarithms of transmission of different steps of the scale in the regions 1 to 5 relatively to the logarithm of transmission of the first step of the scale were deduced. If we express the transmission in percentage and put for the first step of the scale $I_1/I_0 = 100\%$, we can write,

$$\log \frac{I_n}{I_0} = 2 - a_{\lambda n} \qquad (1)$$

with $a_{\lambda n} = k_\lambda x_n$, where k_λ denotes the extinction coefficient at the wave length λ, and x_n the thickness of the n-th layer.

Using the measured values of $a_{\lambda n}$ we can find such relative values of k_λ and x_n, that the product $k_\lambda x_n$ were as close as possible to the measured $a_{\lambda n}$. This task was solved graphically and thus we get the corrected values

Table 3

Logarithms of transmission of the steps of the photometric scale

Step \ Spectral region	1 (H_α)	2 ($D_{1,2,3}$)	3 (H_β)	4 (H_γ)	5 ($H+K$)
1	2·000	2·000	2·000	2·000	2·000
2	1·795	1·812	1·807	1·802	1·796
3	1·630	1·661	1·651	1·643	1·632
4	1·455	1·501	1·487	1·473	1·458
5	1·290	1·350	1·331	1·314	1·294
6	1·100	1·176	1·152	1·131	1·104
7	0·935	1·024	0·997	0·971	0·940
8	0·778	0·881	0·849	0·820	0·784
9	2·000	2·000	2·000	2·000	2·000

Publishing House of the Czechoslovak Academy of Sciences • Provided by the NASA Astrophysics Data System

1959BAICz..10..149V

distance from the centre of the profile, f_k the collimator focal length, and s' the slit width.

As was already shown in the 7th paragraph, the normal width of the slit is different for different spectral regions. When we compare the formula (6) in par. 7 with the relation (8) for σ, we observe that the values of k given in the last column of Table 6 are proportional to the quantity σ, which determines the form of the instrumental profile,

$$k = \frac{\sigma}{\pi} . \qquad (9)$$

A detailed treatise of the instrumental profile will be given later. In this paper we only show as an example the instrumental profile of the Ne lines $\lambda\lambda$ 6533 and 6599, made for region No 1 (H_α). For these lines the values of σ/π are 0·945 and 0·936 and the theoretical instrumental profile for both the lines is almost identical.

This theoretical profile together with the empirical one are shown in Fig. 5. The measured profile shows a considerable symmetry. Observable differences between the two wings can be found only below 5% of the central intensity. Also the profiles in other spectral regions are very symmetrical, which fact testifies the good quality of the grating.

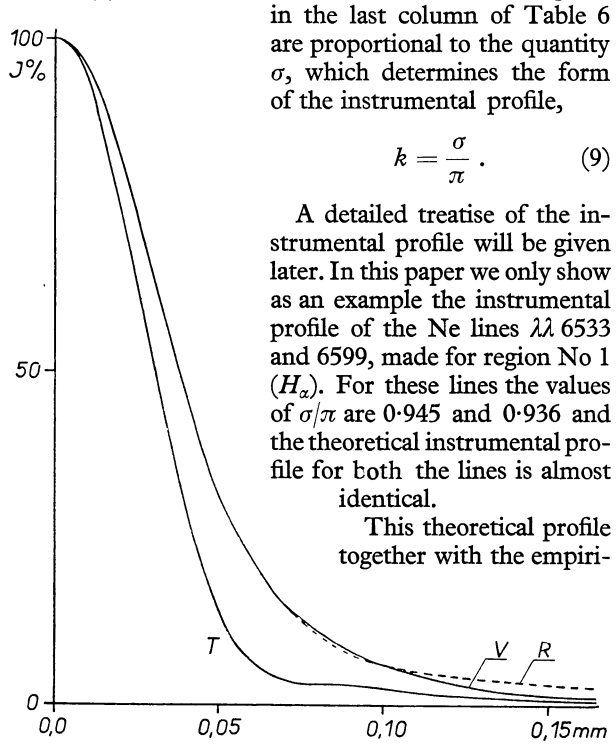

Fig. 5. Relative instrumental profile for the neon lines $\lambda\lambda$ 6532, 6599: V = violet wing, R = red wing of the measured profile, T = theoretical course. (The spectral region No. 1 — H_α).

The half width of the theoretical profile is 60 mÅ, while for the measured profile we find the value of 75·6 mÅ. Thus the empirical profile is about 23% broader. This difference seems to be due only to the proper width of the Ne lines used, because the Doppler half-width of an isotopically pure neon at temperature of 450 °K [10] is about 22 mÅ. Also this problem will be discussed more in detail in another paper which is now being prepared.

9. Ghosts

The intensity of Rowland ghosts was measured in the spectral regions 1, 2 and 4, using the krypton line λ 4319 and the neon lines $\lambda\lambda$ 6599, 6533, 5945, 5882 and 5852. Kr or Ne lamps were placed close in front of the slit and the slit was widened to 1 mm. In this way we got very broad spectral lines with a practically rectangular profile, so that it was possible to determine the total intensity of ghosts irrespectively of the form of the instrumental profile. The ascertained total intensity of ghosts in percentage of the basic line-intensity is given in Table 7. The distances of ghosts were deduced from photographs of the instrumental profile.

Table 7

Spectral region	Intensity of ghosts (%)				Distance of ghosts (Å)	g
	1st order		2nd order			
	red	blue	red	blue		
1	0·75	0·82			4·43	0·0154
2	1·45	1·47	0·12	0·11	3·89	0·0305
4	1·17	1·15			2·86	0·0227

All measurements were made in the second order of the spectrum. Lyman's ghosts were not found. The intensity of ghosts depends on the wave-length in a similar way as the concentration of light (maximum in the surrounding of the region of H_β).

If I denotes the true total intensity of the emission line and gI the total intensity of all ghosts, then the observed intensity of the emission line is $I_1 = (1 - gI)$. If $gI = \varkappa I_1$, then $g = \varkappa/(1 + \varkappa)$. The measured intensities of ghosts give the values of $\varkappa$, and from these values we can calculate the resulting values of g, which are shown in the last column of Table 7.

10. Scattered Light

A given place of a photographic plate in the spectrograph is illuminated not only by the light corresponding to the due wave-length and due part of the solar image on the slit, but also by a certain amount of light, which may be generally denoted as "scattered light". This scattered light can be divided in two main groups:

(a) Scattered light in front of the slit of the spectrograph, in consequence of which the spectrum of the point of the solar disc imaged on the slit is superposed by the spectrum of the total solar disc. This kind of scattering originates partly in the earth's atmosphere, partly on the surfaces of the mirrors and on dust particles present in the space in front of the proper spectrograph. Usually the first part is predominant and, if a special precision is required, the effect of atmospheric scattering must be studied separately for every individual case. Another source of scattered light in this group is due to secondary reflexions caused by the planparallel glass in front of the slit. In consequence of such reflexions the slit is illuminated partially also by light coming from other parts of the solar disc. The intensity of this secondary illumination does not exceed 1% of the primary light falling on the slit.

(b) Scattered light behind the slit of the spectrograph, which may be due to several different reasons:

(1) Scattering due to the grating and imaging objectives along the dispersion.

(2) Scattering due to the grating and imaging objectives along the spectral lines.

(3) Parasite reflexions on optical surfaces.

(4) Superposition of light of different orders.

Publishing House of the Czechoslovak Academy of Sciences • Provided by the NASA Astrophysics Data System

1959BAICz..10..149V

pattern of the slit on the collimator by means of an approximate relation

$$s = 2m\lambda \frac{f_k}{b}, \qquad (5)$$

where m denotes the order of the diffraction minimum considered.

The minimum loss of light requires that the distance between the first minima of the diffraction pattern of the slit be equal to the width of the beam ($b = a$, $m = 1$). Then

$$s = 2\lambda \frac{f_k}{a} = 2s_0 . \qquad (6)$$

This value of s represents the maximum admissible value of the width, useful especially for stronger lines. Its values in different spectral regions are shown in Table 6.

Table 6

Spectral region		λ	$s \cdot 10^2$ mm	k
1	(H_α)	6570	11·15	0·957
2	($D_{1,2,3}$)	5890	10·01	1·066
3	(H_β)	4860	8·26	1·325
4	(H_γ)	4340	7·37	1·447
5	($H+K$)	3930	6·67	1·599
7	(H_∞)	3650	6·20	1·723

It is evident that, with regard to the dependence of s on λ, the width of the slit must not exceed the minimum value of s in the third column of Table 6, as long as we intend to work in all 7 spectral regions. On the other hand, our aim of short exposure-times does not permit us to go much below this limit. With regard to these requirements we have used for the exposures of flares the width $s' = 5{\cdot}34 \cdot 10^{-2}$ mm, (which corresponds to the screw position $x = 28$). The ratio between the used and normal width of the slit, $s'/s_0 = k$, is shown in the last column of Table 6.

8. *Instrumental Profile*

Studying the instrumental profile we must try to observe the same conditions as at exposures of the solar spectrum, primarily the same light conditions in the spectrograph. Therefore, we used the following imaging system: an objective of about 120 cm focal length imaged the source of light top on the slit of the spectrograph. A field lense of about 200 cm focal length was placed in front of the slit to image the newly installed objective on the grating, to conform to the conditions existing at normal exposures of the solar spectrum.

The empirical determination of the instrumental profile is usually made by means of extremely narrow lines of krypton. As, hovewer, we were limited to the chosen spectral regions of individual cameras, we were compelled to use not only krypton but also narrow neon lines. The list of the lines used to our work is as follows:

Region 1 (H_α):	Ne λ 6533, λ 6599
Region 2 ($D_{1,2,3}$):	Ne λ 5852, λ 5882, λ 5945
	Kr λ 5871
Region 4 (H_γ):	Kr λ 4319, λ 4320

In the 3rd region the Ne lines $\lambda\lambda$ 4827 and 4885 were almost invisible even after long exposures, and in the 5th region no intensive krypton and neon lines exist at all.

As the source we used gaseous discharge tubes of neon and krypton of about 20 Torr. pressure. These tubes were fed from a supply of d. c. high voltage of 5 kV.

To be able to measure the instrumental profile even in its wing parts, where the intensity decreases to about 1 per cent of the central intensity of the line, the profile must be composed of several parts. Therefore, we used the following method: first of all, we exposed on every plate the spectrum of Ne or Kr in the given spectral regions without any photometric scale as a control of the illumination of the slit by the neon- or krypton-lamp. After that, we exposed on the same plate the emission Ne- or Kr-lines, using different exposure times and with the photometric scale in front of the slit. These exposures were made for two different widths of the slit: $5{\cdot}34 \cdot 10^{-2}$ mm, and a smaller one, $3{\cdot}39 \cdot 10^{-2}$ mm. The series of photographs on each plate was concluded by another control exposure without the scale. This method has the advantage that the characteristic curve can be constructed for each separate exposure.

To get also the very far wings of the instrumental profile without extremely long exposures, we photographed the Kr or Ne lamp in a position perpendicular to the slit without the photometric scale. To be able to reduce these photographs we made them on the same plate as the preceding ones (made with the lamp parallel to the slit), and choose an exposure-time equal to the longest time used at the photographs made with the scale.

Constructing the instrumental profile we used the same plates and mode of development as for the photographs of the solar spectrum. (Cf. par. 4.) Thus the effects of photographic emulsions and photographic process were also taken into consideration. The exposure times were gradated from several minutes for the central core up to four hours for the extreme wings of the lines.

A Zeiss self-recording microphotometer was used for the evaluation of the plates. The width of the image of the slit on the emulsion was equal to $7 \cdot 10^{-3}$ mm, so that it may have been neglected. Granulation of the plates made no difficulties. The relation of the plate-shift to the movement of the record was controlled by means of a milimeter scale engraved on glass.

The theoretical course of the instrumental profile is determined by the Fraunhofer diffraction of light at an opening given by the size of the grating and can be expressed in the form,

$$I = \text{const} \int_{\alpha-\sigma/2}^{\alpha+\sigma/2} \left(\frac{\sin t}{t}\right)^2 \mathrm{d}t , \qquad (7)$$

where

$$\alpha = \pi m N \frac{\Delta\lambda}{\lambda} ,$$

and

$$\sigma = \pi \frac{a}{f_k} \frac{s'}{\lambda} . \qquad (8)$$

In these relations m denotes the order of the spectrum, N the total number of lines, λ the wave length, $\Delta\lambda$ the

Publishing House of the Czechoslovak Academy of Sciences • Provided by the NASA Astrophysics Data System

1959BAICz..10..149V

of $a_{\lambda n}$, i. e. also the corrected logarithms of transmissions of the steps of the scale. These corrected values of $\log (I_n/I_0)$ are assembled in the above Table 3. The mean error of these corrected values, determined from the differences, $(a_{\lambda n})_{\text{corr.}} - (a_{\lambda n})_{\text{meas.}}$, is $\pm$ 0·002.

6. *Calibration of the Slit*

The slit of the spectrograph has a maximum useful height of 50 mm and it opens symmetrically. The rotation of the micrometer screw opening the slit was coordinated with the varying width of the slit by an interference method. The slit was illuminated from the front by a beam of parallel rays, their divergency being less than 2′. The monochromatic light was produced by an interference filter, with the maximum transmittance at $\lambda = 6370 \pm 44$ Å. The diffraction pattern behind the slit was exposed on Agfa Spektral Rot Rapid Plates, placed at a distance of 49·15 cm from the slit. On the whole, we gained exposures for 8 positions of the micrometer screw. All measurements were evaluated by means of a recording microphotometer, three photometric tracings being in every plate: one corresponding to the centre of the slit and the two other at a distance of 14 mm from the central position, to get information about the parallelism of the edges of the slit.

Let λ denote the wave length of the transmitted light, l the distance of the slit from the plate, and d_m the distance between successive maxima (minima) of the m-th order of the interference pattern on the plate. Then the width of the slit s is for small angles, which come here into consideration, given by the relation,

$$s \frac{d_m}{A_m} = 2\lambda l \quad \text{for} \quad m \neq 0 \tag{2}$$

with $A_m = m$ for the minima. For the maxima, A_m must fulfil the equation $\operatorname{tg} \pi A_m = \pi A_m$. For all photometric tracings a weighted mean of the values of d_m/A_m was calculated, with the value of A_m as the weight of individual measurements.

Then the width of the slit results as

$$s = 2\lambda l \frac{\Sigma A_m}{\Sigma d_m} . \tag{3}$$

The ascertained values of the measured width of the slit (for its centre) in dependence on the setting of the micrometer screw are given in the following Table 4.

Table 4

Setting of the screw	s . 10^2 mm	Mean error (. 10^2 mm)	Number of measured values d_m
25	4·000	0·008	6
30	6·424	0·010	8
35	8·840	0·016	12
40	11·080	0·018	12
50	15·941	0·027	14
65	23·377	0·026	12
80	30·817	0·031	24

The resulting dependence of the slit width, s (in 10^{-2} mm), on the setting of the micrometer screw, x, was found by the method of least squares in the form

$$s = 0{\cdot}4889x - 8{\cdot}3461 .$$

The actual mean error of the setting of the slit width, however, is greater than the error of measurement given in Table 4, because it is determined primarily by the uncertainty in the setting of the screw, which amounts to about $\pm$ 0·1 value of the screw division. Thus we find the actual mean error equal to

$$\Delta s = \pm 0{\cdot}049 \,.\, 10^{-2} \text{ mm} .$$

As the photometric tracings show, the edges of the slit are not exactly parallel, but the slit is slightly broader in its upper part. The diffference of the slit width above and under its centre, $s_a - s_u$, corresponding to a slit height of 28 mm, is shown in the following Table 5.

Table 5

Setting of the screw:	25	30	35	40	50	65	80
$(s_a - s_u)$ . . 10^2 mm:	0·137	0·124	0·133	0·130	0·155	0·226	0·007

7. *Determination of the Optimum Width of the Slit*

In comparison with common types of spectrographs working with one single camera in a limited range of the spectrum, the choice of the optimum width of the slit in our spectrograph is substantially more complicated. First of all, the task of our spectrograph is to follow active processes on the sun, predominantly flares, and this task needs extremely short exposure-times. Consequently, the slit should be as broad as possible. On the other hand, however, we must try to make full use of the resolving power of the grating. This leads to a requirement of a narrow slit, to reduce the influence of the width of the slit on the instrumental profile.

The first requirement can be fulfilled without any difficulty for the Balmer lines, where the form of the instrumental profile is unimportant. In case of middle-strong and faint lines, however, which appear reversed at great chromospheric flares, the instrumental profile plays an important role, and a small width of the slit is quite necessary for any study of these lines.

The normal width of the slit is defined as

$$s_0 = \lambda \frac{f_k}{a} \tag{4}$$

where λ denotes the wave-length, f_k the collimator focal length and a the effective width of the beam passing out of the collimator, in our case equal to the size of the grating, $a = 100$ mm. It is necessary, however, to take into account the light-gathering power of the instrument, which includes the loss of light due to the diffraction at the slit causing an inhomogeneous distribution of light on the collimator. The width of the slit, s, is connected with the distance of the minima, b, in the diffraction

Publishing House of the Czechoslovak Academy of Sciences • Provided by the NASA Astrophysics Data System

1959BAICz..10..149V

(5) Diffuse scattering on the grating, optical surfaces, dust particles, and walls of the spectrograph.

(6) Scattering in the photographic emulsion.

To reduce the influence of diffuse scattering on dust particles on the optical path between the slit and the grating, this whole path has been put in tubes. Short tubes of 150 cm length are also placed in front of every plate holder to suppress any possible parasite side-light coming to the plates. Light of other orders is almost fully eliminated by coloured filters or, moreover, by zero sensitivity of photografic emulsions to the light of undesirable wave lengths. Of course, the used filters in front of the cameras become another source of scattering due to secondary reflexions on their surfaces.

In our spectrograph, the described interior sources of scattered light manifest themselves in the following ways:

(1) Light of a certain wave-length is not concentrated by the grating and objective exactly on one place of the plate, but it comes also to the surrounding of its theoretical wave-length. This scattering consists of two components: the first one is given by the existence of ghosts and the second by the instrumental profile. Both these components have already been discussed above. The correction of the measured values with regard to the ghosts will be explained ad (5).

(2) Scattering along the spectral lines may be due to two reasons: diffraction on the horizontal delimination of the beam of rays, and astigmatism. The astigmatism comes into consideration only in those spectral regions which are imaged by extra-axial pencils of rays, that means close to the right or left border of each imaged region of the spectrum. In our case we found an astigmatic imaging on the plate No. 5 only ($H + K$ region), at the extreme borders of the plate. In other regions this effect does not occur.

Scattering in the direction along the lines was measured in the region No. 2 on the plates used in the discussion on ghosts, which contained exposures of the emission Ne lines. In this case the influence of the total diffused light in the spectrograph can be neglected. Using the broad slit, imaging spectral lines in a rectangular form, the course of intensity of the scattered light along the lines in various distances from the border of the spectrum can be assumed the same as for the spectrum of the sun. The following Table brings the ascertained values of the light scattered perpendicularly to the dispersion, in percentage of intensity of the spectrum.

Table 8

Distance from the border of the spectrum (mm)	0·2	0·4	0·6	0·8	1·0	1·5	2·0
Intensity of the scattered light (%)	0·56	0·35	0·19	0·14	0·10	0·06	0·04

(3) The main source of scattered light at auto-collimating spectrographs is the reflexion on the front surface of the objective before the grating. This source does not exist in our arrangement. A rather intensive reflexion appears on the front surfaces of the objectives $O_1 - O_6$; the reflected light, however, falls predominantly on the walls of the spectrograph, where it is almost fully absorbed. The very small portion of the light reflected from the objectives which falls directly on the photographic plates, causes practically a homogeneous illumination of the whole plate, and its intensity is proportional to the total illumination of the grating in manner analogical to that of diffused scattering, so that this light can be included into the total diffused light as one of its components discussed ad (5).

By a reflexion at the inner surfaces of the filters placed in front of the plates there appears another image of the spectrum, which is shifted in the direction perpendicular to the dispersion, because the filters are slightly inclined towards the optical axis, not to be a source of interference phenomena. The intensity of such a parasite image amounts to 0·2 up to 0·7% of the proper spectrum.

(4) It has already been mentioned that the influence of light of other orders is practically fully eliminated by means of filters and the selectivity of plates.

(5) The total diffused light inside the spectrograph originates by scattering on dust particles, walls of the spectrograph, unhomogeneous surface of the mirrors and the grating. To that we can add also the undesirable reflexions on surfaces of the objectives as mentioned ad (3). Any direct influence of the scattering originating on the collimator and on the mirror M_2 is practically suppressed by means of the tubes between the collimator and the grating.

The total intensity of the diffused light is proportional to the illumination of the grating, and consequently it depends both on the total spectral range coming from the slit and on the total height of the illuminated slit. The illumination by the diffused light may by considered as homogeneous in each imaged region of the spectrum.

Let us express all intensities in the spectrum units of continuum at a chosen wave length, the real intensity of which is I_0. If the slit is illuminated by the solar light, the intensity of the diffused light in the considered spectral region is βI_0, where β is a function of the height of the illuminated slit. The real intensity I in an arbitrary point in the considered region of the spectrum is then given by the relation (cf. [3])

$$\frac{I}{I_0} = r = \frac{r_1(1+\beta) - (g+\beta)}{1-g}, \qquad (10)$$

where r_1 is the observed relative intensity for a given height of the illuminated slit and g is taken from Table 7. For stronger lines, whose width is greater than the distance of ghosts, formula (10) must be somewhat modified.

The value of β can be determined either directly by measuring the intensity of the scattered light in a certain distance from the border of the spectrum, if the component mentioned ad (2) is subtracted, or indirectly by determination of a dependence of the observed central intensity r_1 of an absorption line on the height of the

Publishing House of the Czechoslovak Academy of Sciences • Provided by the NASA Astrophysics Data System

1959BAICz..10..149V

illuminated slit. If r_1 is a linear function of the height of the slit l (in mm), then

$$\beta = \frac{\alpha l}{1 - \alpha l} \approx \alpha l . \qquad (11)$$

To get the coefficient α we made 12 exposures of the spectrum of the centre of the solar disc, for 6 different heights of the slit (from 2 to 20 mm). We measured central intensities of the lines given in Table 9, and found the most suitable linear dependence of r_1 on l by the method of the least squares. Using an extrapolation for $l = 0$ we obtained the central intensities corrected with regard to scattered light (i. e. for $\beta = 0$) and using (10) the real central intensities corrected with regard to the scattered light and the ghosts. Finally using the dependence of r_1 on l we can determine also the coefficient α in the equation (11). The following Table 9 presents central intensities of the measured lines, corrected as to the scattered light and ghosts (not however, as to the instrumental profile), values of the coefficient α, and the values of β determining the scattered light for the usually used height of the slit, $l = 20$ mm.

Table 9

Spectral region	Measured line	Relative central intensity r	Referred to the continuum at λ	$10^2\alpha$	$10^2\beta$
1	H_α	0·159 ± 0·002	6563·0 (interpolated)	0·139	2·86
2	D_1 D_2	0·070 ± 0·003 0·059 ± 0·003	5884·5	0·126	2·58
3	H_β	0·178 ± 0·009	4867·8	0·390	8·46
4	H_γ	0·127 ± 0·003	4332·0	0·109	2·23
5	K	0·047 ± 0·002	3914·8	0·044	0·88

The values of g were taken from Table 7. For the region No. 3 we used the most probable value of $g = 0{\cdot}0305$ and for the region No. 5 we put $g = 0$ with regard to the low intensity in the surrounding of the centre of the K line.

To find out the origin of the scattered light we make several other tests, which showed that there are two most substantial components: one coming to the photographic plate directly from the grating, and another one, originating in the close vicinity of the photographic plate, due to reflexions between the emulsion surface and inner walls of the plate-holder.

(6) Scattering of light in the photographic emulsion depends on the quality and characteristics of the plates, and it is in no direct connection with the proper spectrograph. Therefore we did not study this question in detail. As far as the scattering in emulsion can influence the measured results, this influence must be studied individually for different kinds of used plates. Its influence on profiles of spectral lines is usually included in the discussion of the instrumental profile, as it is one of the reasons of differences between the observed and calculated profiles of the line.

The different components of the scattered light discussed above make themselves important in different ways when creating the resulting intensity of light, which causes the blackening on photographic plates. Details of intensity distribution along the dispersion are distorted owing to their surrounding by the form of the instrumental profile and scattering in the emulsion. Details of intensity along the lines are influenced by the diffraction phenomena on the borders of the spectrum, reflection on filters in front of the plates, and scattering in the emulsion.

Besides these effects which distort details in the spectrum there is also the influence of the total diffused light and ghosts. As to these two components, the corrected intensity can be found using the relation (10).

11. Acknowledgement

Our thanks are due to Prof. E. R. Mustel of the Crimean Astrophysical Observatory, U. S. S. R., for several helpful discussions when constructing the inner equipment of the spectrograph.

REFERENCES

[1] *R. S. Richardson, R. Minkovski:* ApJ 89 (1939), 347.
[2] *C. W. Allen:* MN 100 (1940), 635.
[3] *M. A. Ellison:* Publ. Royal Obs. Edinburgh 1 (1952), 75.
[4] *Z. Suemoto:* Publ. Astr. Soc. Japan 3 (1951), 110.
[5] *Z. Švestka:* Publ. Astr. Inst. Czech. Acad. Sci. No. 32 (1957).
Z. Švestka: BAC 7 (1956), 130.
Z. Švestka, L. Fritzová: BAC 8 (1957), 61.
[6] *E. R. Mustel, A. B. Severny:* Izv. Krym. A. O. 8 (1952), 19.
[7] *A. B. Severny:* Izv. Krym. A. O. 17 (1957), 129.
T. V. Kasachevskaja, A. B. Severny: Izv. Krym. A. O. 19 (1958), 46.
A. B. Severny: Izv. Krym. A. O. 19 (1958), 72.
T. V. Kasachevskaja: Izv. Krym. A. O. 20 (1958), 80.
[8] *R. Michard, R. Servajean, J. Laborde:* ApJ 127 (1958), 504.
[9] *Ch. Moore:* Princeton Contr. No. 20 (1945).
[10] *W. Priester:* ZfA 32 (1953), 228.

Publishing House of the Czechoslovak Academy of Sciences • Provided by the NASA Astrophysics Data System